Food Bioscience 74 (2025) 108013

Contents lists available at ScienceDirect

Food Bioscience

journal homepage: www.elsevier.com/locate/fbio

Effect of pulsed electric field parameters on peptide migration selectivity and efficiency in whey protein hydrolysate separation by electrodialysis with ultrafiltration membrane

Leonel C. Mafotang T. [a,b,c], Aurore Cournoyer [a,b], Jacinthe Thibodeau [a,b], Marcello Fidaleo [c,*], Laurent Bazinet [a,b,**]

[a] Institute of Nutrition and Functional Foods (INAF), Université Laval, Quebec City, QC, G1V 0A6, Canada
[b] Department of Food Sciences and Laboratoire de Transformation Alimentaire et Procédés ElectroMembranaires (LTAPEM, Laboratory of Food Processing and ElectroMembrane Processes), Université Laval, Quebec City, QC, G1V 0A6, Canada
[c] Department for Innovation in Biological, Agro-Food and Forest Systems, University of Tuscia, Viterbo, Italy

ARTICLE INFO

Keywords:
Electrodialysis with ultrafiltration membrane
Pulsed electric field
Mass transfer efficiency
Duty cycle
Concentration polarization
Electroconvective vortices

ABSTRACT

In this study, we investigated the influence of pulsed electric field (PEF) conditions during electrodialysis with ultrafiltration membrane (EDUF) on the separation of peptides present in a whey protein hydrolysate (WPH). Six PEF conditions, defined by different pulse/pause durations (1s/1s, 5s/1s, 5s/5s, 10s/1s, 10s/5s, 10s/10s) were compared. Peptide migration efficiency (MR_{charge}) and selectivity were evaluated in both cationic and anionic recovery compartments. The duty cycle (pulse duration divided by total cycle time) emerged as a key parameter, with lower values consistently associated with higher peptide migration efficiency. These effects arise from the combined action of concentration polarization (CP) relaxation during pauses and short-lived electroconvective vortices (ECVs) generated at the start of each pulse. Furthermore, PEF conditions affected peptide selectivity, likely due to the dynamic competition among charged peptides within the diffusion boundary layer (DBL), since repeated pulse-pause cycles affect DBL extension and concentration profile formation, favoring the transport of larger or less mobile peptides. Altogether, these results provide new insights into how mechanisms well established in conventional electrodialysis (ED) also govern peptide transport in EDUF and that tuning the duty cycle can strategically improve peptide migration efficiency.

1. Introduction

Industrial biofood streams such as whey, blood and wastewater are complex, protein-rich matrices produced in very large volumes. Globally, around 180–190 million tons of whey are generated annually, with projections of 203–241 million tons by 2030 (Buchanan et al., 2023). Such by-products represent both an environmental burden and an opportunity since enzymatic hydrolysis of their protein fraction can release diverse peptide mixtures with a wide range of bioactivities, including antioxidant, antihypertensive, antibacterial (Arrutia et al., 2016) and therefore high added-value potential. Valorization of whey through peptide recovery thus represents an attractive circular economy (Li-Chan, 2015; Zaky et al., 2022). However, industrial implementation is hampered by the difficulty of selectively separating peptides, which often share similar physicochemical properties (Fernández et al., 2013).

Conventional membrane separations such as ultrafiltration and nanofiltration offer scalability but discriminate primarily by size, limiting peptide-level selectivity (Bazinet & Firdaous, 2013; Belfort, 2019). Electrodialysis with ultrafiltration membranes (EDUF) provides an advantage by combining charge selectivity of ion-exchange membranes with size exclusion of ultrafiltration membranes (Alavi & Ciftci, 2023). This hybrid mechanism has been used to separate peptides from blood, milk and other hydrolysates (Cournoyer et al., 2024; He et al., 2016). More recently (Cournoyer et al., 2024, 2025), studied the effect of different current modes: continuous current (CC), PEF and polarity reversal (PR) on the migration selectivity of peptides from a porcine blood hydrolysate during electrodialysis with ultrafiltration membrane. These studies demonstrated for the first time that the electrical current

* Corresponding author. Department for Innovation in Biological, Agro-Food and Forest Systems, University of Tuscia, Viterbo, Italy.
** Corresponding author. Institute of Nutrition and Functional Foods (INAF), Université Laval, Quebec City, QC, G1V 0A6, Canada.
E-mail addresses: fidaleom@unitus.it (M. Fidaleo), laurent.bazinet@fsaa.ulaval.ca (L. Bazinet).

https://doi.org/10.1016/j.fbio.2025.108013
Received 10 October 2025; Received in revised form 25 November 2025; Accepted 26 November 2025
Available online 29 November 2025

modes and conditions have effects on the mass transfer and final peptide profiles in the recovery compartment. Indeed, three groups of current conditions with similar performances were identified: CC, PEF with 10 s pulse followed by 1 s pause (10s/1s) and PR with the same pulse/pause duration (10s/1s) promoted the selective migration of cationic peptides with low molecular masses. Despite the chosen cationic configuration of the system (allowing only the recovery of cationic peptides), PR 1s/1s facilitated the migration of some anionic peptides due to short polarity reversal, while PEF 1s/1s exhibited intermediate behavior. However, the chosen PEF conditions (10s/1s and 1s/1s) were not enough to fully elucidate the underlying mechanisms involved in EDUF under PEF process on peptide migration selectivity.

Few studies have demonstrated the positive impacts of PEF in conventional electrodialysis (ED) systems (Lemay et al., 2019; Mishchuk et al., 2001; Ruiz et al., 2007). These works showed that applying PEF can reduce concentration polarization (CP), limit membrane fouling and enhance mass transfer, leading to improved demineralization efficiency and lower specific energy consumption compared to CC. In EDUF, (Suwal et al., 2016) were the first to apply PEF and PR using a snow crab by-product hydrolysate, demonstrating that both modes mitigated fouling and water dissociation while PEF also led to lower energy consumption compared to CC. However, their study focused primarily on amino acid migration, leaving the mechanisms governing peptide migration selectivity largely unexplored. Building on these findings, (Cournoyer et al., 2024, 2025) provided the first direct evidence that the electrical current modes significantly influence peptide migration selectivity during EDUF. Nevertheless, the mechanistic basis of these effects, particularly how specific PEF parameters modulate mass transfer efficiency and peptide migration selectivity, remains poorly understood.

Mechanistically, these selectivity shifts may arise from CP and transient diffusion boundary layer (DBL) dynamics. Indeed, in multicomponent ED, species with lower mobility or larger size are disproportionately impacted by CP and electrostatic interactions, leading to competitive hierarchies within the DBL (Zimmermann et al., 2023). In ED under PEF, periodic CP relaxation during pauses can redistribute species concentrations, while current surges and ECVs at pulse onset create transient gradients. These conditions, in EDUF, may alter which peptides reach the membrane surface, favoring some over others depending on charge, size or diffusivity (Cournoyer et al., 2024, 2025). However, systematic peptide-level evidence of such mechanisms in EDUF remains scarce.

In this context, the aim of the present study was to explore different PEF conditions to allow a more comprehensive study of their impact on peptide migration efficiency and selectivity during fractionation of a whey protein hydrolysate. The specific objectives were to (1) assess the impact of different PEF conditions on peptide migration efficiency, (2) to identify and characterize peptides, and (3) to study their impacts on peptides selectivity.

2. Materials and methods

2.1. Whey protein hydrolysate

The whey protein hydrolysate (WPH) used in this study was prepared from Prolacta 95, a whey protein isolate containing 90 % (w/w) protein (Lactalis, Retiers, France). To produce the hydrolysate, 444 g of Prolacta 95 was dissolved in 20 L of deionized water, yielding a 2 % (w/v) solution and allowed to solubilize overnight at 10 °C under gentle stirring. Enzymatic hydrolysis was conducted for 3 h at 37 °C and pH 2.5 (Guo et al., 1995) using pepsin at an enzyme-to-substrate ratio of 1:40 (Damen et al., 2024). The pH was maintained with 3 M HCl. Following hydrolysis, the solution was heated to 80 °C for 15 min to inactivate the enzyme (Geoffroy et al., 2022). The resulting WPH was divided into aliquots and stored at −30 °C for subsequent EDUF experiments.

2.2. Peptides separation in electrodialysis with ultrafiltration membrane

EDUF separations were carried out using an MP-type electrodialysis cell (ElectroCell AB, Täby, Sweden) with an effective membrane surface area of 100 cm^2. The cell was assembled with a food-grade anion-exchange membrane (AMX-fg), a cation-exchange membrane (CMX-fg) and two polyethersulfone ultrafiltration membranes (50 kDa MWCO, Synder Filtration, Vacaville, CA, USA), positioned near the anode (FM1) and cathode (FM2) (Fig. 1). The system included four recirculation loops connected to external tanks. The feed compartment contained 600 mL of 2 % (w/v) WPH circulated at 700 mL/min. The anionic and cationic recovery compartments each held 600 mL of KCl solution (2 g/L), also circulated at 700 mL/min. The electrode rinsing compartments contained 1000 mL of Na_2SO_4 (20 g/L) circulated at 800 mL/min. Centrifugal pumps (CL3503, Baldor Electric Company, Arkansas, USA) ensured continuous circulation, with flow rates monitored and controlled by flow meters (F-550, Blue-White Industries Ltd., CA, USA).

Before running the separation experiments, the limiting current density (LCD) of the system was determined through preliminary duplicate experiments following Cowan and Brown (Cowan & Brown, 1959), resulting in an LCD of 102 A/m^2 (1.02 A). Voltages were applied under potentiostatic control using a 0–30 V power supply (HQ Power PS3003, Xantrex, Burnaby, BC, Canada) and a multimeter monitored the applied voltage directly at the electrodes. Six PEF conditions were tested, varying both pulse and pause durations: 1s/1s, 5s/1s, 5s/5s, 10s/1s, 10s/5s, and 10s/10s (Table 1). During each pulse a constant voltage of 7.8 V was applied, while during the pause the voltage returned to 0 V, generating currents between 0.436 and 0.607 A using a Pulsewave 760 generator (Bio-Rad Laboratories, Richmond, BC, Canada). Each treatment applied 2 h of effective current, leading to different total durations depending on the pulse/pause combination (Martí-Calatayud et al., 2021). The temperature was continuously monitored throughout the runs, although not actively controlled. Across all experiments, the temperature variations between the start and the end of each run averaged 11.18 ± 1.26 °C. This variation was consistent among conditions, indicating that any thermal effect, if present, would have similarly affected all treatments. The randomized order of the experiments further minimized potential bias due to temperature fluctuations. A schematic diagram of the EDUF setup, including membrane configuration, recirculation loops, and electrode placement is provided in Fig. 1. To facilitate comparison among PEF conditions, the duty cycle (α) and the frequency (Hz) were also considered, as they provide a more comprehensive description of the pulsing pattern. The duty cycle (α) was determined using equation (1) (Malek et al., 2013; Sistat et al., 2015), and corresponds to the portion of time the current is active during each cycle:

$$\alpha = t_{pulse} / (t_{pulse} + t_{pause}) \quad (1)$$

Where t_{pulse} and t_{pause} in second (s) represent the time in which the current was applied, or not, during a PEF signal. The frequency (Hz) is defined as the number of times the PEF signal repeats in 1 s (Salam & Rahman, 2018).

It is important to note that PEF used in this study refers to the application of low-voltage, time-modulated electrical field during electromembrane separation. This approach differs fundamentally from the high-intensity PEF (typically >1 kV/cm) used for electroporation or microbial inactivation (Lytras et al., 2024). The voltages applied here (7.8 V corresponds to 2 V/cm) are far below electroporation thresholds, and the objective was to modulate peptide migration, CP and ECVs phenomena rather than to induce membrane permeabilization or cellular effects.

2.3. Total peptide concentration analysis

Peptide concentrations in the anionic and cationic compartments

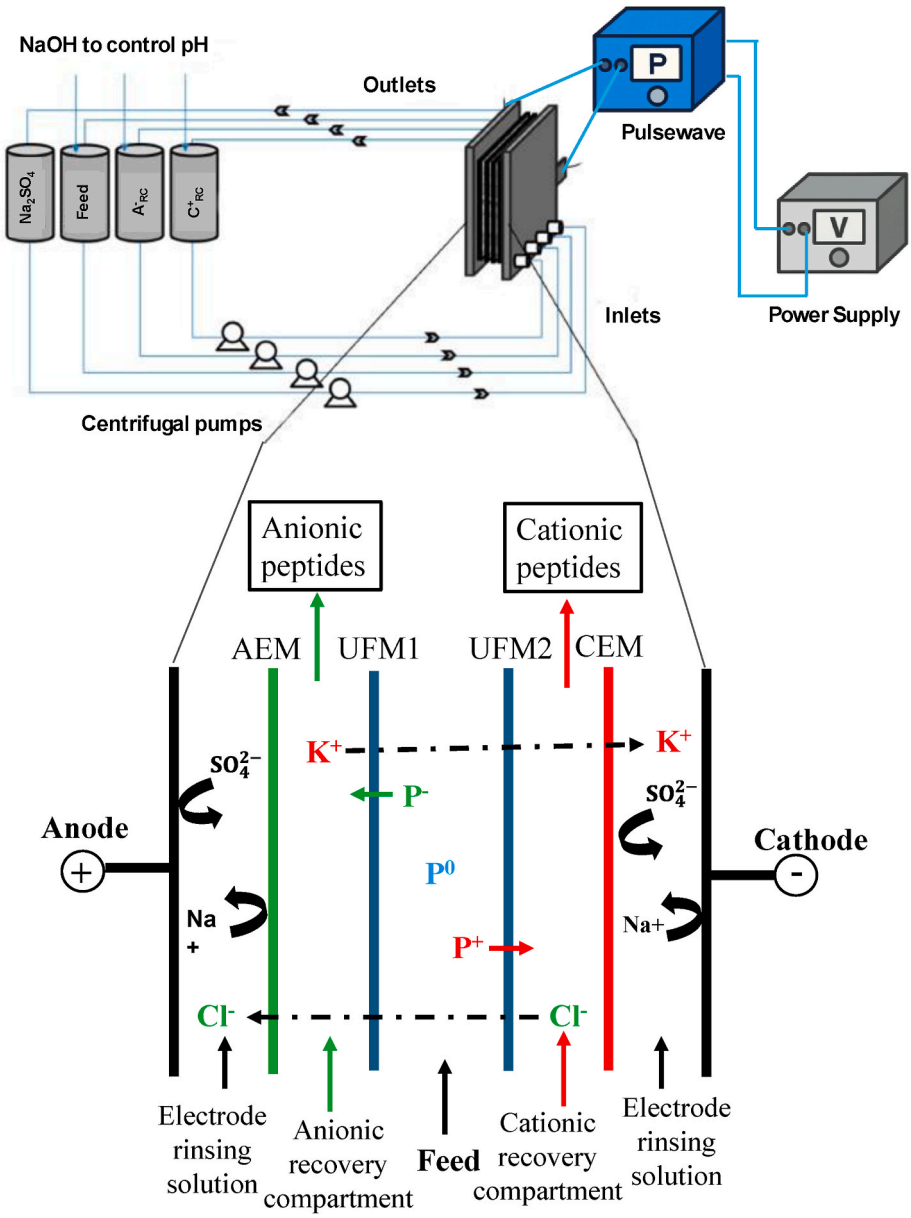

Fig. 1. Schematic diagram and cell configuration of the electrodialysis with ultrafiltration membrane system for the simultaneous separation of anionic and cationic peptides obtained from whey protein hydrolysate. FM1 and FM2: filtration membranes with same molecular weight cut-off; AEM: anion-exchange membrane; CEM: cation-exchange membrane; P^+: cationic peptide; P^-: anionic peptide; P^0: neutral peptide (adapted from Suwal et al., 2017).

Table 1
Pulsed electric field conditions considered in this study.

PEF condition	Pulse duration (s)	Pause duration (s)	Ratio pulse/pause	Process duration (h)	Duty cycle (−)	Frequency (Hz)
1s/1s	1	1	1	4	0.5	0.50
5s/1s	5	1	5	2.4	0.83	0.17
5s/5s	5	5	1	4	0.5	0.10
10s/1s	10	1	10	2.2	0.91	0.09
10s/5s	10	5	2	3	0.67	0.07
10s/10s	10	10	1	4	0.5	0.05

were quantified using the μBCA Protein Assay Kit (Thermo Fisher Scientific, Waltham, MA, USA) following the manufacturer's protocol. Absorbance at 562 nm was measured after 2 h incubation at 37 °C with an xMark Microplate Spectrophotometer (Bio-Rad, Mississauga, ON, Canada).

2.4. UPLC-MS/MS analyses: peptide migration and selectivity

2.4.1. UPLC-MS/MS method

Peptide identification in the recovery EDUF fractions under each PEF condition was performed using UPLC-MS/MS. The chromatographic and mass spectrometry setup was the same as previously described by (Cournoyer et al., 2024; Damen et al., 2024), based on a 1290 Infinity II

UPLC system coupled to a 6560 IM-Q-TOF mass spectrometer (Agilent Technologies, Santa Clara, CA, USA). In this study, hydrolysate samples (2 % w/v) were filtered through 0.45 μm PVDF filters and 10 μL were injected into an Infinity Lab Poroshell 120 EC-C18 column (2.1 mm × 100 mm, 2.7 μm, Agilent, CA, USA). Separations were carried out at 45 °C with a flow rate of 0.4 mL/min and a maximum operating pressure of 600 bar. The mobile phases consisted of solvent A (LC-MS grade water with 0.1 % formic acid) and solvent B (LC-MS grade ACN with 0.1 % formic acid). The gradient was optimized for peptides migration analyses, starting at 1 % B, ramping to 45 % B over 30 min, followed by a 2-min step at 95 % B and a 3-min cleaning at 100 % B before re-equilibration. MS data were acquired in positive mode and analyzed with Mass Hunter BioConform Software (Agilent Technologies), using the same calibration and acquisition parameters as in (Cournoyer et al., 2024; Damen et al., 2024).

2.4.2. Data treatment and statistical analysis

The recovered fractions from all EDUF experiments were analyzed using the Agilent Mass Hunter Software package (Agilent Technologies, Santa Clara, CA, USA). Initially, MS-spectra and UV-chromatograms were acquired using LC/MS Data Acquisition Version B.08.00. Through a visual comparison of the UV chromatograms obtained for the different PEF conditions, the most important peaks from cationic and anionic compartments were selected, focusing on those that varied the most in terms of height between conditions. These peaks were considered representative of peptides that either migrated preferentially or exhibited condition-dependent differences. The concentration factor (CF, see Section 2.4.3) of each peak was then statistically compared across PEF conditions using one-way ANOVA, followed by Tukey's pairwise multiple comparison test ($p < 0.05$). Only peaks that showed significant differences between PEF conditions were considered for further analysis.

The peptide sequences corresponding to each peak were identified using MS-spectra, and analyzed with BioConfirm Software (Version 10.0, Agilent Technologies). Biomolecules were matched to known protein sequences present in the Prolacta hydrolysate, including beta-lactoglobulin, alpha-lactalbumin, bovine serum albumin, and caseins (alpha S1, S2, beta, and kappa). In addition, research was cross-referenced with several bioactive peptide databases (BioPep, AHTPDB, DFBP, PlantPep and PepLab). For each identified peptide, the amino acid sequence, molecular mass (Da), and position within the specific protein sequence were determined. Only peptides reproducibly detected in at least two of the three experimental replicates were retained for further analysis (Cournoyer et al., 2024). These reproducible peptides were then used as markers to compare peptide migration across the different PEF conditions. Finally, a principal component analysis (PCA) was performed on the selected peaks, to study the general behavior of PEF conditions on peptide migration.

2.4.3. Migration and migration selectivity of peptides

To assess the efficiency of the electric charge transported through the electrodes to drive peptide migration, the migration rate based on charges transported was introduced as Eq. (2):

$$MR_{charge} = m_{peptides} / (S{\cdot}C) \quad (2)$$

Where MR_{charge} is expressed in g/m^2·C, $m_{peptides}$ the mass of peptides in gram (g), S is the ultrafiltration membrane surface (0.01 m^2) and C the number of charges transported in Coulomb (C) (Cournoyer et al., 2024). The mass of peptides ($m_{peptides}$) used in Eq. (2) was determined from the peptide concentrations quantified as described in Section 2.3. Briefly, the peptide concentration (μg/mL) in each compartment at the end of the experiment was multiplied by the corresponding solution volume (mL) and the resulting value was converted to grams using the factor 10^6, according to Eq. (3):

$$m_{peptides} = (C_{peptides}.\ V) / 10^6 \quad (3)$$

The effect of the separation on peptide migration was studied by introducing the concentration factor of each peptide (CF_i), defined as the ratio of the final peak concentration in the recovery compartment to that in the initial hydrolysate in the feed compartment before EDUF, as follows (Dushkova et al., 2023):

$$CF_i\ (\%) = (C_{iR} / C_{iF}) \text{ x } 100 \quad (4)$$

Where the index i indicates the specific peak of interest, while C_{iR} and C_{iF} represent the area under the curve of the peak in the recovery and feed compartments, respectively, as measured from UV chromatogram. This parameter expresses the peptide enrichment in the recovery compartment compared to the feed and is thus proportional to peptide migration.

The selectivity of peptide migration was defined for each peptide i with respect to peptide j as the ratio of the CF of peptide i to that of peptide j (Wang et al., 2022):

$$S_{i,j} = \frac{C_{i,R}/C_{i,F}}{C_{j,R}/C_{j,F}} = CF_i \Big/ CF_j \quad (5)$$

The first part of Eq. (5) suggests that the selectivity can be interpreted as the ratio between the abundance, obtained from UV chromatogram of species i (relative to j) in recovery and that in the feed compartment. In Eq. (5), the reference peak for each recovery compartment was chosen as the one with the lowest CF among the selected peaks.

3. Results and discussion

3.1. Efficiency of mass transfer

From the final peptide concentrations data, the efficiency of peptide migration (MR_{charge}) was determined. In the C^+_{RC} (Fig. 2a), assessing the impact of pulse duration, 1s/1s led to a higher MR_{charge} than 10s/1s, while no significant difference was observed with 5s/1s ($p = 0.147$). For the pause duration, 10s/10s showed the highest MR_{charge}, followed by 10s/5s while condition 10s/1s had the lowest MR_{charge}. Regarding the impact of the frequency, the MR_{charge} in 10s/10s was significantly higher than in 1s/1s. In the A^-_{RC} (Fig. 2b), assessing the impact of pulse duration, 1s/1s resulted in a significantly higher MR_{charge} than 5s/1s ($p = 0.018$) and 10s/1s ($p = 0.028$). For the pause duration, MR_{charge} was higher in 10s/10s than in 10s/1s ($p = 0.030$), while no significant difference was observed compared to 10s/5s ($p = 0.426$). Finally, for the impact of the frequency, the MR_{charge} in 5s/5s was significantly higher than in 1s/1s and 10s/10s. These results confirm that the MR_{charge} is influenced by the studied PEF conditions and in most cases, it increases as α decreases. A similar trend was previously reported by (Cournoyer et al., 2024, 2025), who compared CC, PEF and PR conditions during the EDUF of a porcine cruor hydrolysate. The authors observed that, for the same total duration of electric field application, the 1s/1s PEF condition ($\alpha = 0.5$) resulted in a significantly higher migration rate than 10s/1s ($\alpha = 0.91$) and CC ($\alpha = 1$) for cationic peptides. The present results extend these findings by including broader range of PEF conditions and examining both anionic and cationic recovery compartments, confirming that lower α values systematically lead to higher efficiencies.

To better illustrate this relationship, MR_{charge} was plotted as a function of α for both compartments (Fig. 3). The resulting curves clearly show an inverse correlation, where MR_{charge} increases as α decreases. This graphical representation reinforces the conclusion that lower duty cycles promote more efficient peptide migration under PEF operation.

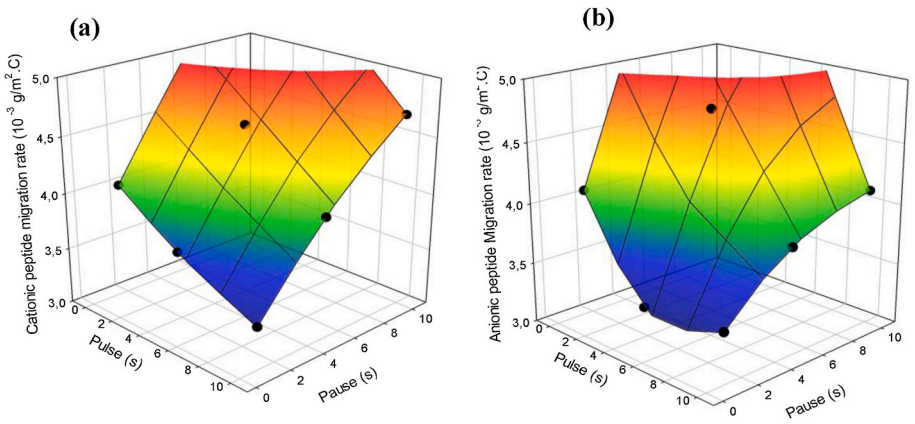

Fig. 2. MR_{charge} as a function of pulse and pause in (**a**) cationic recovery compartment and (**b**) anionic recovery compartment for the six pulsed electric field conditions.

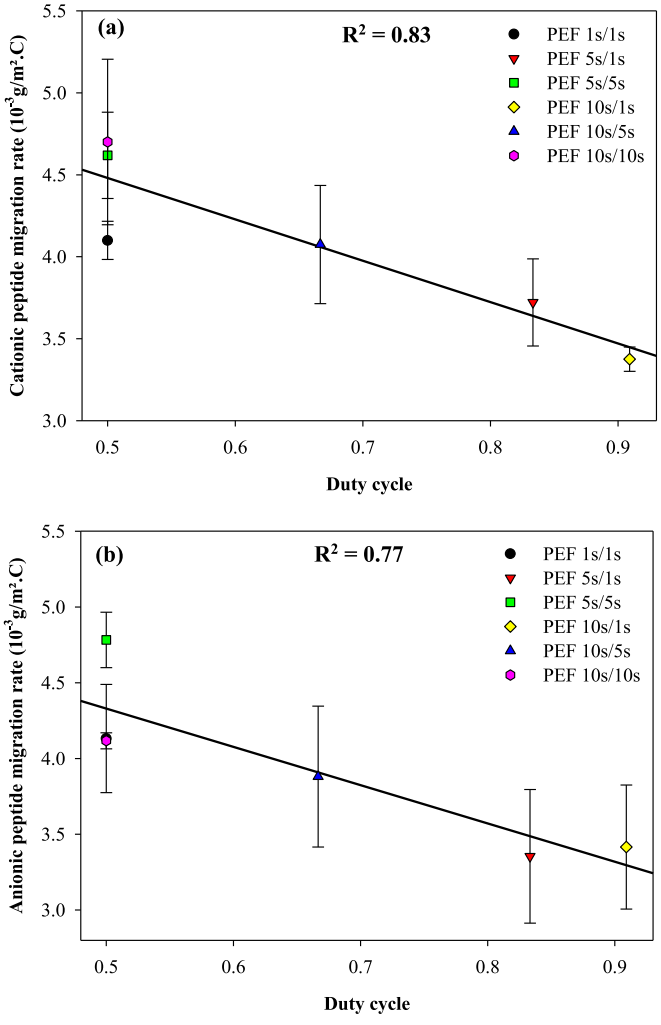

Fig. 3. Relationship between the mass transfer efficiency and the duty cycle in (**a**) cationic and (**b**) anionic recovery compartments during electrodialysis with ultrafiltration membrane. Continuous lines represent linear regression fits.

3.2. Peptide population in the recovery fractions

3.2.1. Analyses of UV chromatograms

Following UPLC-MS/MS analyses, UV chromatograms were generated for each recovery compartment and compared to the initial WPH chromatogram under identical injection conditions (2 % w/v protein concentration). To facilitate the identification of peptides recovered under the different PEF conditions, chromatograms of the feed solution and the recovery compartments were combined by charge type: Fig. 4 presents the results for the C_{RC}^{+} and Fig. 5 for the A_{RC}^{-}. From these chromatograms, 22 prominent peaks in C_{RC}^{+} and 20 in A_{RC}^{-} were selected and labeled as key regions for the analysis of peptide migration differences observed in the experiment. Variations in peak height across chromatograms demonstrated that the extent of peptide migration and the selectivity of migration changed as a function of the studied PEF conditions. These chromatographic shifts are consistent with earlier EDUF studies that directly linked operating mode to differential peptide recovery. In particular (Suwal et al., 2017), compared *in situ* and *ex situ* enzymatic protein hydrolysis and separation in EDUF and reported that during *in situ* hydrolysis, almost all peaks in the feed chromatogram were reduced in height and area compared to the corresponding *ex situ* controls, reflecting peptide migration from the feed compartment toward the anionic and cationic recovery compartments. Importantly, by analyzing peptide profiles and migration rates across compartments, the authors observed that certain peaks in the *ex situ* experiment migrated to a greater extent than their corresponding peaks in the *in situ* condition. Moreover, some peaks present in the recovery compartments during the *ex situ* experiment were absent under *in situ* experiment.

The selected peaks were then integrated in the C_{RC}^{+}, A_{RC}^{-} and in the initial WPH to determine their concentration factor (CF) (see Eq. (4)) and consequently assess the process selectivity. The statistical analysis revealed significant differences across PEF conditions. Specifically, 8 peaks in C_{RC}^{+} and 7 peaks in A_{RC}^{-} were found to be statistically different ($p < 0.05$), highlighting variations in peptide migration under the tested conditions (Table 2).

In the C_{RC}^{+}, the pulse duration influenced the CF values across different peaks. Specifically, 1s/1s led to a significantly higher CF for peak 14 compared to 5s/1s and 10s/1s, whereas 5s/1s resulted in a significantly lower CF than 1s/1s and 10s/1s for peaks 16 and 18. Regarding the pause duration, 10s/1s showed a significantly lower CF than 10s/10s for peaks 10, 12, 14, and 18, as well as compared to 10s/5s for peak 16. Finally, in terms of frequency, 10s/10s had a significantly lower CF than 5s/5s for peak 8, while the opposite was observed for peak 11. In addition, based on the observed results, it appears also that in the C_{RC}^{+}, apart from peaks 8 and 11, where conditions 5s/5s and 10s/10s showed significant differences, no significant differences were observed among the conditions with α value of 0.5 (1s/1s, 5s/5s, and 10s/10s) across the other peaks. In contrast, for the other peaks, the observed differences were predominantly between the conditions with higher α values of 0.83 and 0.91 (10s/1s and 5s/1s respectively) or with an intermediate α value of 0.67 (10s/5s) and at least one condition with α of 0.5. This trend is particularly evident for peak 18, where the CF showed

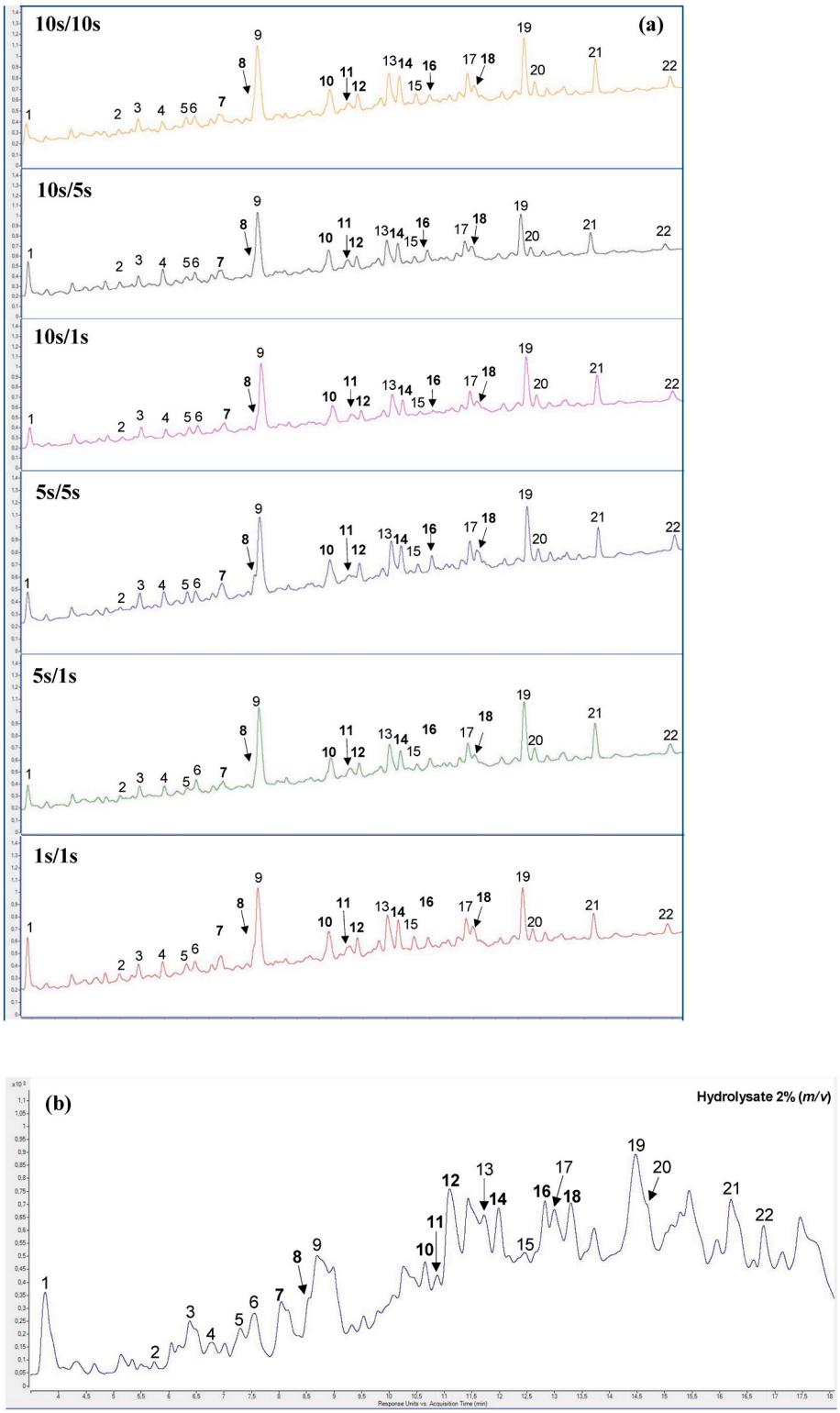

Fig. 4. UV-chromatograms of the (**a**) cationic recovery compartment at the end and (**b**) corresponding feed solution (WPH) at the beginning of electrodialysis with ultrafiltration membrane process for the six PEF conditions.

a 2.7-, 2.97- and 2.51-fold increase under conditions 1s/1s, 5s/5s and 10s/10s respectively, compared to conditions 5s/1 or 10s/1s. Similarly, for peak 16, the CF showed a 2.98-, 3.53- and 2.88-fold increase under conditions 1s/1s, 5s/5s and 10s/10s respectively, compared to 10s/1s (Table 2).

In the $A_{\overline{RC}}$, the pulse duration also had an impact, with 1s/1s showing a significantly higher CF for peaks 2, 16, and 17 compared to 5s/1s and 10s/1s; for peaks 5 and 10 compared to 10s/1s; and for peak 6 compared to 5s/1s. For the pause duration, 10s/1s resulted in a significantly lower CF than 10s/10s for peak 16. Finally, considering the frequency, 5s/5s showed a significantly higher CF than 10s/10s for peak 6. This trend observed in the $A_{\overline{RC}}$ is similar to that observed in the C^{+}_{RC}, where the main differences occurred between at least one of the conditions with a higher α value and at least one of the conditions with an α value of 0.5.

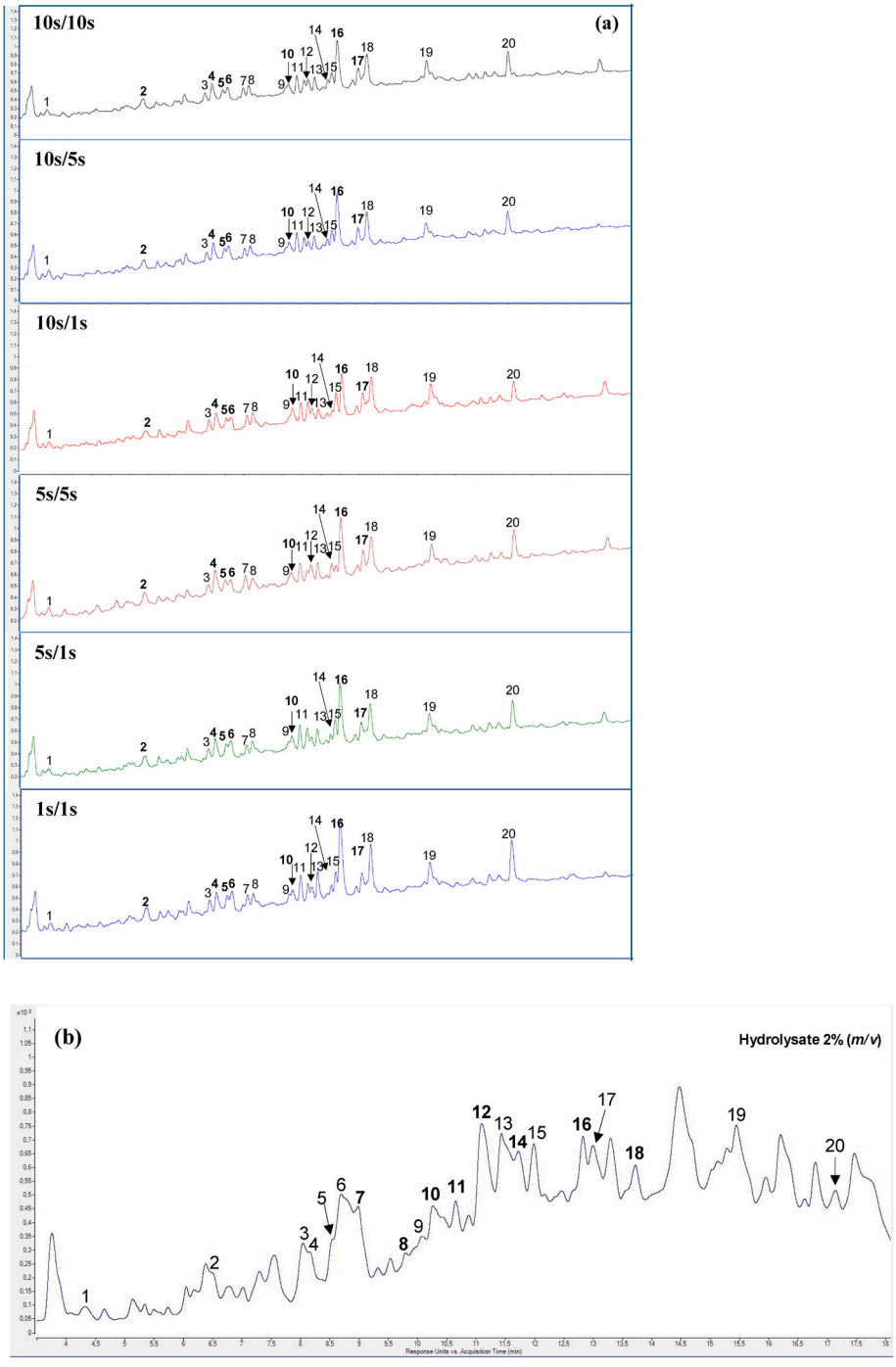

Fig. 5. UV-chromatograms of the (**a**) anionic recovery compartment at the end and (**b**) corresponding feed solution (WPH) at the beginning of electrodialysis with ultrafiltration membrane process for the six PEF conditions.

Specifically, the CF for peak 6 showed a 3.02- and 1.88-fold increase under conditions 1s/1s and 5s/5s respectively, compared to 5s/1s.

This trend, already observed in the MR_{charge} (process efficiency), confirms that PEF conditions affect the peptide migration, and that migration improves as the α decreases, since higher CF values were observed for PEF conditions with lower α values (1s/1s, 5s/5s and 10s/10s). Since both selectivity and CF were defined based on peaks, and each peak may contain a group of co-eluting peptides rather than a single peptide, the resulting values reflect the behavior of peptide families rather than individual peptides.

3.2.2. *Impact of PEF conditions on peptide migration*

Principal component analysis (PCA) was applied to the CF data to facilitate the study of the effects of PEF conditions on peptide migration. For both compartments, the three repetitions of each condition were represented with 95 % confidence ellipses to see if the groups were distinct or overlapped in the PCA score plot (Zhu et al., 2014), helping to understand how data clustered and how the conditions were related to one another. The first principal component (PC1) explained a large portion of the total variance in peptide migration data, with 57.8 % and 72.0 % for C^{+}_{RC} and A^{-}_{RC} respectively. When considering both PC1 and PC2, more than 75 % and 85 % of the total variance were explained in C^{+}_{RC} and A^{-}_{RC} respectively, thus providing a good representation of the

Table 2
Concentration factor of selected peaks as a function of pulsed electric field conditions for the cationic and anionic compartments for the six PEF conditions.

Peak		Retention time (min)[a]	Concentration factor (%)[b]												p-value
			1 s/1 s		5 s/1 s		5 s/5 s		10 s/1 s		10 s/5 s		10 s/10 s		
			Avg	sd	Avg	sd	Avg	sd	Avg	sd	Avg	sd	Avg	sd	
Cationic compartment	7	8.78	**10.21** ^{a,b}	1.56	**6.22** ^{a}	1.06	**11.83** ^{b}	1.50	**7.54** ^{a,b}	1.86	**7.90** ^{a,b}	1.10	**9.84** ^{a,b}	3.17	0.029
	8	9.53	**7.12** ^{a,b}	0.67	**5.15** ^{a}	1.18	**7.95** ^{b}	0.36	**5.31** ^{a}	0.65	**6.04** ^{a,b}	0.67	**5.60** ^{a}	0.67	0.003
	10	11.22	**26.99** ^{a,b}	4.47	**24.06** ^{a,b}	1.59	**31.30** ^{a,b}	2.20	**20.98** ^{a}	4.74	**27.61** ^{a,b}	2.05	**32.36** ^{b}	2.82	0.008
	11	11.65	**17.59** ^{a,b}	4.29	**16.17** ^{a,b}	1.33	**5.28** ^{a}	2.31	**14.33** ^{a,b}	4.26	**15.02** ^{a,b}	7.77	**18.50** ^{b}	4.19	0.039
	12	11.86	**1.89** ^{a,b}	0.35	**1.43** ^{a,b}	0.22	**1.71** ^{a,b}	0.21	**1.23** ^{a}	0.03	**1.61** ^{a,b}	0.16	**1.97** ^{b}	0.17	0.010
	14	12.80	**8.39**^{b}	1.17	**5.85** ^{a}	0.41	**7.90** ^{a,b}	0.11	**5.59** ^{a}	0.21	**6.93** ^{a,b}	1.45	**8.89** ^{b}	1.12	0.003
	16	13.49	**6.37**^{b}	1.83	**3.01** ^{a}	2.15	**7.55** ^{b}	0.65	**2.14** ^{a}	0.62	**6.47** ^{b}	2.04	**6.17** ^{a,b}	1.01	0.005
	18	14.49	**3.46** ^{b,c}	0.70	**1.28** ^{a}	0.41	**3.80** ^{c}	0.24	**1.28** ^{a}	0.47	**1.93** ^{a,b}	0.64	**3.22** ^{b,c}	0.91	<0,001
Anionic compartment	2	6.88	**15.62** ^{b}	2.04	**10.49** ^{a}	2.18	**15.03** ^{a,b}	1.40	**10.11** ^{a}	1.62	**11.75** ^{a,b}	2.63	**13.13** ^{a,b}	0.70	0.014
	4	8.71	**9.05** ^{a,b}	1.31	**6.97** ^{a}	1.37	**10.40** ^{b}	1.16	**7.15** ^{a}	0.77	**8.23** ^{a,b}	1.09	**9.26** ^{a,b}	0.58	0.016
	5	8.99	**4.19** ^{b,c}	0.78	**2.37** ^{a,b}	0.74	**4.34** ^{c}	0.83	**2.11** ^{a}	0.43	**3.32** ^{a,b,c}	0.77	**3.69** ^{a,b,c}	0.46	0.008
	6	9.53	**3.02** ^{b,c}	0.26	**1.97** ^{a}	0.23	**3.70** ^{c}	0.15	**2.29** ^{a,b}	0.37	**2.53** ^{a,b}	0.54	**2.73** ^{a,b}	0.04	<0.001
	10	10.93	**16.58** ^{b}	0.62	**14.08** ^{a,b}	1.33	**14.16** ^{a,b}	1.68	**12.06** ^{a}	0.81	**14.06** ^{a,b}	2.04	**13.98** ^{a,b}	1.28	0.044
	16	12.56	**11.82** ^{c}	2.41	**7.10** ^{a,b}	1.05	**11.63** ^{b,c}	1.88	**6.80** ^{a}	1.67	**9.65** ^{a,b,c}	1.60	**11.36** ^{b,c}	1.06	0.007
	17	12.78	**30.03** ^{b}	4.04	**17.54** ^{a}	2.72	**29.04** ^{b}	3.56	**18.89** ^{a}	1.83	**21.95** ^{a,b}	4.92	**25.55** ^{a,b}	3.10	0.003

[a] Retention time was averaged for all conditions and their repetitions.
[b] Concentration factor values followed by a different letter for each peak (row) are significantly different using a Tukey multiple comparison test ($p \leq 0.05$) (One-way ANOVA with PEF conditions as treatments).

original data.

For the C^{+}_{RC}, the loading plot (Fig. 6a) shows that most peaks primarily contribute to PC1, except peak 11 which is predominantly associated with PC2. Based on migration correlations, three distinct groups of peaks can be identified: group A including only peak 11; group B with peaks 10, 12 and 14; and group C made up of peaks 16, 18, 7 and 8. In parallel, the score plot (Fig. 6b) reveals a clear separation of several PEF conditions along PC1, without overlapping confidence ellipses. Specifically, regarding the pulse duration, 1s/1s is separated from 5s/1s and 10s/1s, while for the pause duration, 10s/5s is separated from 10s/1s. However, the impact of the frequency does not result in significant separation among the conditions along PC1. Along PC2, 5s/5s is separated from 10s/10s, further highlighting the influence of PEF conditions on peptide migration. PEF conditions located on the positive side of the PC1 are associated with higher migration values for most peptides compared to those on the negative side. This suggests a decreasing trend in peptide migration depending on the PEF condition in the following order: 1s/1s, 5s/5s and 10s/10s, followed by 10s/5s and finally 10s/1s and 5s/1s. Interestingly, PC1, which represents the migration of most peptides, is negatively correlated with the duty cycle, confirming that conditions with lower α value correspond to higher migration. This trend aligns with the previously observed MR_{charge} results (see Section 3.1). On the other hand, the frequency does not show a clear effect in the score plot, as conditions 1s/1s (high frequency) and 10s/10s (low frequency), which share the same α value appear overlapped. However, 5s/5s appears distinctly located relative to other conditions with the same α value, suggesting in this case a potential effect of the frequency.

Similarly, in the A^{-}_{RC}, the loading plot (Fig. 7a) indicates two groups of peaks with correlated migration: group D including peaks 10 and 2 and group E including peaks 17, 5, 16, 6 and 4. The score plot (Fig. 7b) reveals that contrary to the C^{+}_{RC}, the separation of PEF conditions occurs only along PC1. Specifically, regarding the pulse duration, 1s/1s is separated from 5s/1s and 10s/1s, while for pause duration and frequency, no separation without overlapping confidence ellipses is observed. Conditions 1s/1s, 5s/5s and 10s/10s located on the positive side of the PC1 are associated with higher migration values for most of the peptides compared to 10s/1s which is located on the negative side with no overlapping confidence ellipses.

The additional graph of PC1 for both cationic and anionic compartments as a function of α (Fig. 8) further supports the conclusions drawn from the PCA score plots. Since PC1 accounts for most of the variance in peptide migration, following its behavior provides a reliable indicator of the global impact of the PEF conditions. Across compartments, PC1 values decrease as α increases, showing that lower α conditions (1s/1s, 5s/5s and 10s/10s) are systematically associated with higher peptide migration. This trend once again highlights that α is a key factor influencing overall peptide migration, while differences in pulse or pause duration have more subtle effects. The consistent pattern observed in both cationic and anionic compartments reinforces the idea that tuning α can be used strategically to optimize migration efficiency across a range of PEF conditions.

To further interpret the PCA results, the selectivity of each peptide was assessed relative to a reference peak using ANOVA. Peak 12 was considered as reference for C^{+}_{RC} and peak 6 for A^{-}_{RC}. The reference peak for each recovery compartment was chosen as the one with the lowest CF among the selected peaks. The analysis revealed a significant effect of the PEF conditions on the selectivity, specifically, $S_{8,12}$ (selectivity of peak 8 referred to peak 12), $S_{11,12}$ and $S_{18,12}$ in C^{+}_{RC} and $S_{10,6}$ in the A^{-}_{RC} ($p = 0.05$). In the C^{+}_{RC}, the loading plot identified three clusters of correlated CFs (A, B and C). Since peak 12, used as the reference belongs to group B, peaks outside group B were expected to show PEF-dependent selectivity variations. While significant effects were observed for $S_{8,12}$, $S_{11,12}$ and $S_{18,12}$, other potential variations may have not been detected due to data variability and consequent low statistical power. A similar trend was observed in the A^{-}_{RC}, where the PCA loading plot identified two groups of correlated CFs (D and E). Given this clustering pattern, at least one binary selectivity was expected to change with PEF conditions when using peak 6, which belong to group E as a reference. This was confirmed by $S_{10,6}$, corresponding to the peak with the highest contribution to PC2 and the weakest correlation with the reference group, which showed statistically significant variation across PEF conditions.

These differences in selectivity could be better explained by

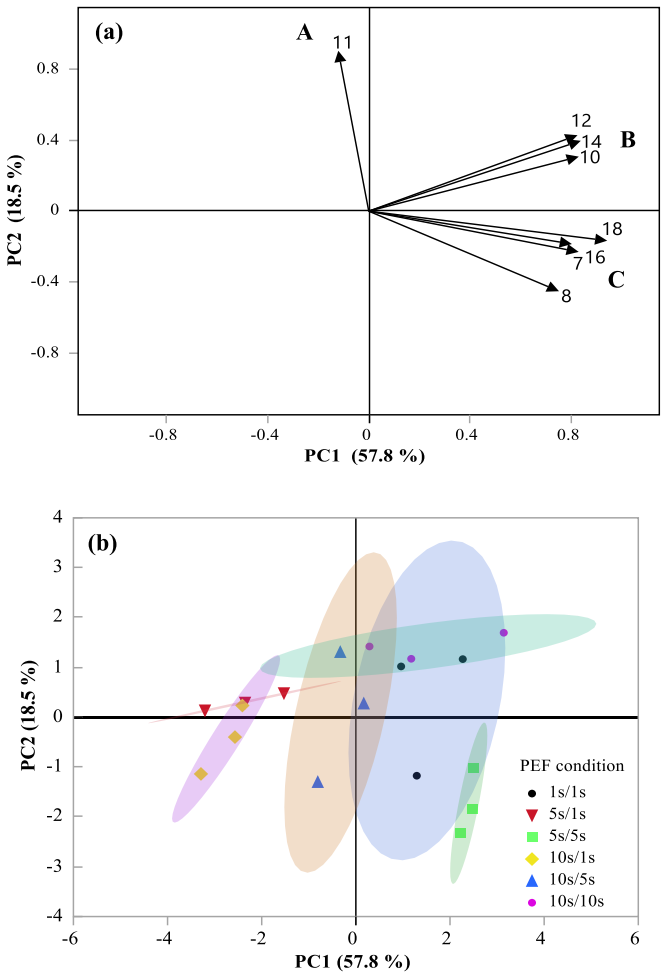

Fig. 6. Principal component analysis (PCA), including (**a**) loading plot and (**b**) score plot, of the 8 selected peaks for the six pulsed electric field conditions tested for the cationic compartment. The shaded areas refer to 95 % confidence ellipses.

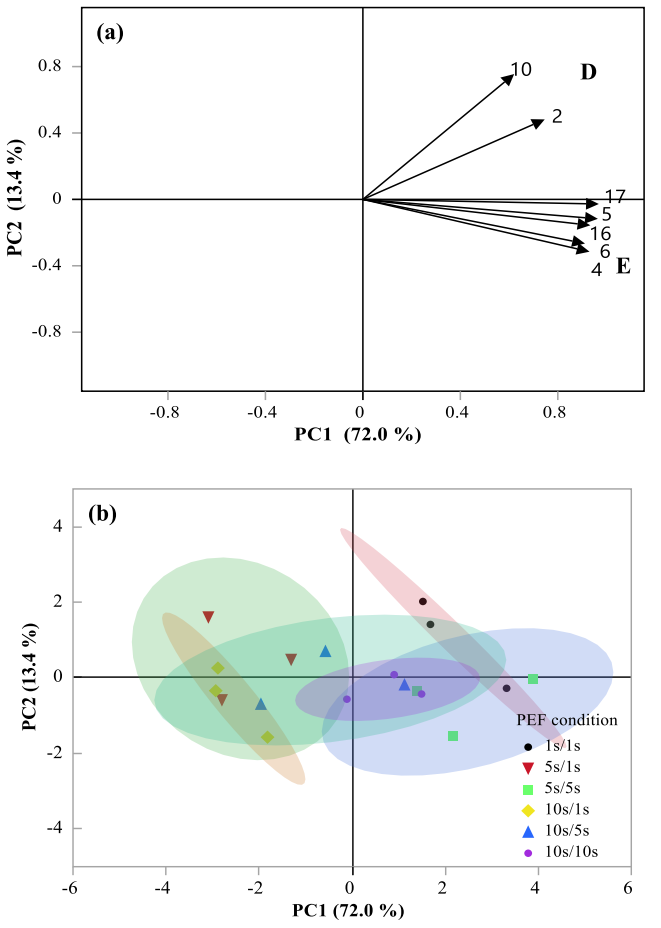

Fig. 7. Principal component analysis (PCA), including (**a**) loading plot and (**b**) score plot, of the 7 selected peaks for the six pulsed electric field conditions tested for the anionic compartment. The shaded areas refer to 95 % confidence ellipses.

considering species-specific interactions within the DBL, as supported by recent work from (Zimmermann et al., 2023) in multicomponent ED systems. In such systems, ions or charged species with lower mobility or larger size are disproportionately impacted by CP and electrostatic interactions, especially when coexisting with faster, smaller counterions. This creates a competitive hierarchy in the DBL, where only the species that maintain sufficient local concentration and exhibit high electrophoretic mobility are efficiently transported. This concept aligns with the theoretical models (Geraldes & Afonso, 2010; Gorobchenko et al., 2022; Zabolotsky et al., 2020), which describe how ion selectivity in multi-ionic systems depends on current density and on each ion's critical current density. According to these models, as the applied current approaches the limiting value for a given species, its boundary concentration tends toward zero and mass transfer becomes dominated by diffusion through the DBL rather than membrane permselectivity. Therefore, when transient or pulsating electric fields are applied, as in PEF-ED, the system repeatedly crosses these transport regimes, alternating between periods dominated by electromigration (during the pulse) and diffusion-controlled recovery (during the pause). Such transitions are expected to dynamically modulate the hierarchy of species competition at the membrane surface.

When extended to EDUF, such competitive effects have been experimentally observed during the separation, where the presence of abundant peptides was shown to affect the migration of specific species through inter-species competition as previously observed by (Langevin et al., 2012; Roblet et al., 2013) on peptides mixture and (Aider et al., 2008) on chitosan oligomers. In the present study, similar interactions are expected within the DBL, where differences in concentration and charged-based interactions dynamically affect each peptide's access to the membrane surface. For instance, during long pause duration when the electric field is off, the concentration gradients near the membrane have time to relax, leading to a more uniform distribution of peptides in the DBL (Cournoyer et al., 2025). This reduces the strong transport advantage typically held by smaller, highly charged and consequently faster peptides under constant field conditions. As a result, larger or less mobile peptides have a better chance to reach the membrane and migrate, shifting the balance of which peptides are transported and thus their selectivity. Moreover, the study emphasizes that electromigration under non-steady conditions (like PEF) causes transient concentration and electric field gradients. These momentary changes affect each peptide species differently depending on their size, charge or diffusivity. So, peptides with similar charges but different molecular weight or hydrophobicity may then respond differently to these transient profiles (Cournoyer et al., 2025).

3.2.3. Identification and characterization of peptides

The peptides present in the peaks (for both the anionic and cationic compartments) highlighted in Table 2 were identified and analyzed in terms of their amino acid sequence, molecular weight, and corresponding whey proteins. Additionally, detailed information about the peptide's presence or absence in these peaks across the different PEF conditions is also provided in Table 3. Bioinformatics tools (Biosynth;

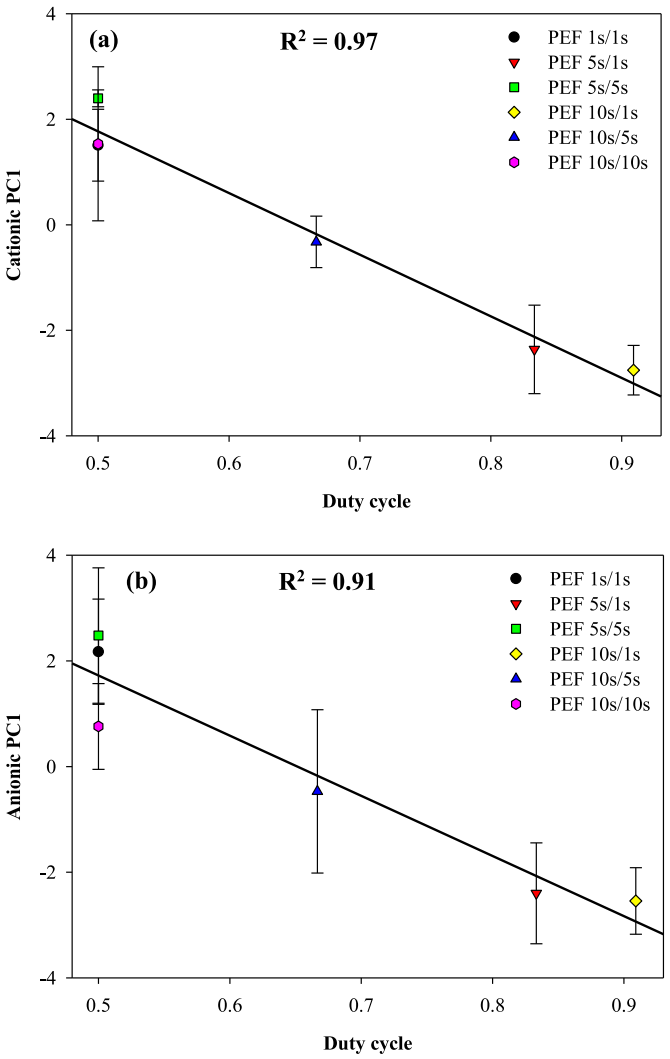

Fig. 8. Effect of duty cycle on global peptide migration in (**a**) cationic recovery compartment and (**b**) anionic recovery compartment for the six pulsed electric field conditions. Continuous lines represent linear regression fits.

(NovoPro)) were used to determine the isoelectric point (pI), net charge at pH 7, GRAVY score, as the average of hydropathy values of amino acid residues, and the percentage of hydrophobic residues. The net charge of the peptides was presented at pH 7 to reflect their charged state during the separation process carried out at pH 7.

In total, 14 peptides were identified in the C_{RC}^{+} with molecular weights ranging from 431.238 Da to 2109.221 Da (Table 4). Among these peptides migrated in the C_{RC}^{+}, 5 had an isoelectric point (pI) below 7, indicating a negative charge, while the remaining peptides were positively charged. Group A from PCA (Fig. 6a) contained a positively charged peptide (NKVLVL). Group B appeared to be a mixture of positively, negatively and neutrally charged peptides, with molecular masses ranging from 583.267 to 1217.670 Da and 80 % of peptides having molecular masses above 800 Da. Group C consisted primarily of positively charged peptides (with only one neutral peptide, GGVSL) and molecular masses ranging from 431.238 to 2109.221 Da, with 75 % of peptides with molecular masses above 800 Da. In the A_{RC}^{-}, 9 peptides were identified with molecular masses ranging from 381.190 Da to 1307.673 Da. All peptides that migrated in the A_{RC}^{-} had a pI below 7, confirming their negative charge. Group D from PCA (Fig. 7a) contained three peptides: VRTPEVDDE, VRTPEVDDEAL and AASDISL, with molecular masses of 1058.488; 1242.610; and 675.344 Da, respectively. Group E appeared to be a mixture, including peptides with low molecular masses (373.221; 381.190; 675.344; 805.395 and 955.509 Da) and higher molecular masses (1058.488; 1157.598; 1242.610 and 1307.673 Da). The migration of negatively charged or neutral peptides, particularly in cationic recovery configuration, has been previously documented in the literature, likely due to electrostatic or hydrophobic interactions forming aggregates with a net positive charge that are able to migrate (Cournoyer et al., 2024, 2025; Faucher et al., 2022; Geoffroy et al., 2022; Kadel et al., 2021).

These identified sequences were compared to the literature reporting active peptide sequences from whey protein and were also tested in databases, including BioPep, AHTPDB, DFBP, PlantPep and PepLab. Among the anionic peptides, peak 2 contained a known binding peptide (VRTPEVDDE), peaks 4 and 5 contained antioxidative peptides (YSL and EIL respectively). Regarding the cationic peptides, no bioactive peptides were identified. However, potential bioactive peptides were identified, with sequences similar to known bioactive peptides, differing only by a few amino acids (Table 5).

To better understand the distribution of peptides observed in the PCA loading plots (Figs. 6a and 7a), an additional PCA was performed on the considered physicochemical characteristics (data not shown). This complementary analysis aimed to identify possible relationships explaining their clustering. Among the considered features, the net charge at pH 7 (and the closely related pI) emerged as the strongest contributors to group discrimination. However, a notable variability in charge was observed within some clusters, particularly in group C where peptide charges ranged from 0 to 3 (Table 4). This suggests that while charge plays an important role in peptide behavior during EDUF, it is not the only determining factor and that other features also have an impact that cannot be fully resolved with the current dataset. From a physicochemical perspective, the apparent influence of charge can be tentatively related to the limiting current density (LCD) concept established in ED theory. Although LCD in this study was experimentally determined for the entire system configuration and not for each peptide species, it nonetheless provides a useful theoretical framework to interpret charge-dependent transport. In ED, the LCD represents the point at which ion migration at the membrane interface is balanced by diffusion from the bulk solution. Theoretical and experimental studies have shown that LCD values are strongly affected by both ionic valence and diffusivity, since these parameters determine how efficiently ions move through the DBL (Tekinalp et al., 2023; Zimmermann et al., 2023). Based on this, charge may influence peptide migration efficiency in a way comparable to diffusivity: a more highly charged peptide can, in principle, carry more current and experience stronger electrostatic driving forces. However, these two parameters are not independent. In complex peptide systems such as EDUF, the transport of charged species cannot be explained only by their charge or diffusivity. A higher charge can sometimes be counterbalanced by lower diffusivity, as larger peptides diffuse more slowly despite carrying higher charge and peptides with comparable charge may still behave differently depending on other characteristics such as MW, sequence length, or 3D structure, all of which can influence mobility through steric and hydrodynamic effects.

4. Global discussion

The efficiency of peptide migration, expressed as MR_{charge}, was strongly affected by PEF conditions and the trends observed can be explained by the interplay between CP relaxation and ECV activity. Regarding pulse duration, MR_{charge} in C_{RC}^{+} was higher under 1s/1s compared to 10s/1s, while no significant difference was observed with 5s/1s. This agrees with the fact that more frequent pulses generate more current surges and ECV events per unit time, reducing CP and favoring peptide transport as previously reported in EDUF by (Cournoyer et al., 2025). In A_{RC}^{-}, the trend was even clearer, with 1s/1s exhibiting significantly higher MR_{charge} than both 5s/1s and 10s/1s.

Regarding the impact of pause duration, under the 10s/1s condition, the system has minimal pause duration between pulses. Although this

Table 3
Peptide presence in peaks across different PEF conditions.

Peak[a]		Peptide sequence	Molecular mass (Da)	Associated protein	Presence in the condition					
					10s/10s	10s/5s	10s/1s	5s/5s	5s/1s	1s/1s
Cationic compartment	7	AQSAPLRV	840.482	β-lactoglobulin	x	x	x	x	x	x
		GGVSL	431.238		x	x	x	x	x	x
	8	YKKYLL	826.496	β-lactoglobulin	x	x	x	x	x	x
	10	LDAQSAPLRV	1068.593	β-lactoglobulin	x	x	x	x	x	x
	11	NKVLVL	684.453	β-lactoglobulin	x	x	x	x	x	x
	12	YSLAM	583.267	β-lactoglobulin	x	x	x	x	x	x
	14	LPMHIRL	878.517	β-lactoglobulin	x	x	x	x	x	x
		SFNPTQL	805.398		x	x	x	x	x	x
		LIVTQTMKGLD	1217.670		x	x	x	x	x	x
	16	PMHIRL	765.433	β-lactoglobulin	X	x	x	x	X	x
		KGLDIQKVAGTW	1314.733			x	x	x		x
		KFDKALKALPMHIRL	1780.062			x	x	x		
		ALPMHIRL	949.555					x		
	18	LEKFDKALKALPMHIRLS	2109.221	β-lactoglobulin	x	x	x	x	x	x
Anionic compartment	2	VRTPEVDDE	1058.488	β-lactoglobulin	x	x	x	x	x	x
	4	EGDLEILLQKW	1307.673	β-lactoglobulin	x	x	x	x	x	x
		YSL	381.190		x	x	x	x	x	x
	5	EIL	373.221	β-lactoglobulin	x	x	x	x	x	x
	6	DAQSAPLRV	955.509	β-lactoglobulin	x	x	x	x	x	x
	10	VRTPEVDDEAL	1242.610	β-lactoglobulin	x	x	x	x	x	x
		AASDISL	675.344		x	x	x	x	x	x
	16	DTDYKKYLL	1157.598	β-lactoglobulin	x	x	x	x	x	x
	17	SFNPTQL	805.395	β-lactoglobulin	x	x	x	x	x	x

[a] N° of peak corresponds to the number of the peak in the UV-chromatograms in Figs. 4a and 5a.

Table 4
Characteristics of peptides identified in the major chromatogram's peaks in each compartment.

	Main peaks	Group	Sequences	Molecular Mass (Da)	Associated protein	Location	Isolelectric point	Net charge at pH 7	GRAVY	Hydrophobic residues (%)
Cationic compartment	7	C	AQSAPLRV	840.482	β-LG	34–41	9.80	1.00	0.15	0.63
	7	C	GGVSL	431.238	β-LG	19–23	5.53	0.00	1.28	0.80
	8	C	YKKYLL	826.496	β-LG	99–104	9.53	1.99	−0.47	0.33
	10	B	LDAQSAPLRV	1068.593	β-LG	32–41	5.84	0.00	0.15	0.60
	11	A	NKVLVL	684.453	β-LG	90–95	8.75	0.99	1.43	0.67
	12	B	YSLAM	583.267	β-LG	20–24	5.52	−0.01	1.08	0.60
	14	B	LPMHIRL	878.517	β-LG	143–149	9.76	1.10	0.67	0.71
	14	B	SFNPTQL	805.398	β-LG	150–156	5.24	−0.01	−0.50	0.43
	14	B	LIVTQTMKGLD	1217.670	β-LG	1–11	6.09	0.00	0.50	0.55
	16	C	PMHIRL	765.433	β-LG	144–149	10.18	1.10	0.15	0.67
	16	C	KGLDIQKVAGTW	1314.733	β-LG	8–19	8.59	0.99	−0.24	0.58
	16	C	KFDKALKALPMHIRL	1780.062	β-LG	135–149	10.29	3.09	−0.02	0.60
	16	C	ALPMHIRL	949.555	β-LG	142–149	9.80	1.10	0.81	0.75
	18	C	LEKFDKALKALPMHIRLS	2109.221	β-LG	133–150	9.70	2.10	−0.04	0.56
Anionic compartment	2	D	VRTPEVDDE	1058.488	β-LG	123–131	4.16	−3.00	−1.38	0.33
	4	E	EGDLEILLQKW	1307.673	β-LG	51–61	4.14	−2.00	−0.30	0.55
	4	E	YSL	381.190	β-LG	20–22	5.52	−0.01	0.57	0.33
	5	E	EIL	373.221	β-LG	55–57	4.05	−1.00	1.60	0.67
	6	E	DAQSAPLRV	955.509	β-LG	33–41	5.84	0.00	−0.26	0.56
	10	D	VRTPEVDDEAL	1242.610	β-LG	123–133	4.05	−3.00	−0.62	0.45
	10	D	AASDISL	675.344	β-LG	25–31	4.05	−1.00	0.97	0.57
	16	E	DTDYKKYLL	1157.598	β-LG	96–104	5.96	0.00	−1.17	0.22
	17	E	SFNPTQL	805.395	β-LG	150–156	5.24	−0.01	−0.50	0.43

*The principal component analysis was used to define groups A, B, C, D and E as outlined below. GRAVY: Grand Average of Hydropathy index. β-LG: β-Lactoglobulin.

allows for more frequent reapplication of the electric field, the 1s pause may not be long enough for the DBL to fully relax or for the ion concentration near the membrane surface to recover sufficiently (Nikonenko et al., 2024). Consequently, even if ECVs are periodically generated, their potential to enhance mass transfer is compromised by the elevated resistance caused by residual CP. This can be supported by numerical simulations by (Uzdenova et al., 2015) suggesting that when pauses are too brief, electroconvection alone cannot maintain enhanced ion transport in overlimiting conditions. This means that even though vortices are forming, their positive effect on peptide migration is limited because there isn't enough time for the system's resistance to recover in this condition (Cournoyer et al., 2025). This is reflected in the lowest MR_{charge} in 10s/1s. As the pause duration increases to 5 s (10s/5s), the system is granted more time to dissipate CP and re-establish favorable ion gradients before the next pulse. This leads to improved current efficiency (Bazinet & Geoffroy, 2020). Additionally (Lemay et al., 2019), emphasized that longer pause intervals allow for better ion replacement in the boundary layer, which lowers local resistance and enhances overall transport efficiency during the subsequent pulse. In the 10s/10s condition, the extended 10 s pause further enhances CP dissipation and facilitates even greater recovery of the depleted ion layers. This leads to the highest observed MR_{charge} in the cationic compartment, and comparable performance to 10s/5s in the anionic compartment. However, the relatively small improvement between 10s/5s and 10s/10s in the

Table 5
Predicted and reported activities of peptide sequences identified in the selected chromatogram peaks.

	Peaks	Identified sequence	Match in Database	Matching (%)	Known and potential activity	Database	Database ID	Ref.
Cationic recovery compartment	7	AQSAPLRV	DAQSAPLRVY	80	Anti-Hypertensive (IC50[a]: 12.2 μM) potential	AHTPDB	2546	Tavares et al. (2011)
	7	AQSAPLRV	DAQSAPLRVY	80	ACE inhibitor potential	BioPep	9112.0	Tavares et al. (2011)
	7	AQSAPLRV	DAQSAPLRVY	80	ACE-inhibitory potential	DFBP	DFBPACEI1039	Tavares et al. (2011)
	7	AQSAPLRV	DAQSAPLRVY	80	ACE inhibitor potential	PepLab	PL59	Tavares et al. (2011)
	12	YSLAM	WYSLAM	83	Anti-Hypertensive (IC50 : 56.3 μM) potential	AHTPDB	6965	Hernandez-Ledesma et al. (2007)
	12	YSLAM	WYSLAM	83	antioxidative potential	BioPep	7903.0	Hernandez-Ledesma et al. (2007)
	12	YSLAM	WYSLAM	83	(ACE-inhibitory peptides, Multifunctional peptides, Antioxidative peptides) potential	DFBP	DFBPANOX0294	Hernandez-Ledesma et al. (2007)
Anionic recovery compartment	6	DAQSAPLRV	DAQSAPLRVY	90	Anti-Hypertensive (IC50 : 12.2 μM) potential	AHTPDB	2546	Tavares et al. (2011)
	6	DAQSAPLRV	DAQSAPLRVY	90	ACE inhibitor potential	BioPep	9112.0	Tavares et al. (2011)
	6	DAQSAPLRV	DAQSAPLRVY	90	ACE-inhibitory potential	DFBP	DFBPACEI1039	Tavares et al. (2011)
	6	DAQSAPLRV	DAQSAPLRVY	90	ACE inhibitor potential	PepLab	PL59	Tavares et al. (2011)
	5	**EIL**	**EIL**	**100**	**Antioxidative**	DFBP	DFBPANOX0874	Tian et al. (2015)
	5	**EIL**	**EIL**	**100**	**ACE-inhibitor**	PlantPep	PPepDB_3136	Gu and Wu (2013)
	2	**VRTPEVDDE**	**VRTPEVDDE**	**100**	**binding**	BioPep	10183.0	Caetano-silva et al. (2015)
	2	VRTPEVDDE	LVRTPEVDDE	90	binding potential	BioPep	10172.0	Caetano-silva et al. (2015)
	4	**YSL**	**YSL**	**100**	**Antioxidative**	DFBP	DFBPANOX0839	Tian et al. (2015)
	4	**YSL**	**YSL**	**100**	**Antioxidant**	PlantPep	PPepDB_3714	X. Wang et al. (2017)

[a] IC50: concentration of the peptide (in micromolar, μM) required to inhibit 50 % of the target activity. Sequences in **bold** represent those with known bioactivities.

anionic compartment suggests a saturation point in recovery benefits. This is consistent with findings by (Rubinstein & Zaltzman, 2000), who noted that beyond a certain relaxation threshold, the conventional ED system's recovery is essentially complete, and further increases in pause duration did not lead to additional benefit.

Finally, regarding the impact of frequency (1s/1s, 5s/5s and 10s/10s), the resulting differences can be explained by considering the competing effects of ECVs and the restauration of the depleted concentration near the membrane surface during the pause, as well as the interactions between them. From the perspective of ECV effect, shorter pulses are more favorable. The 1s/1s condition, where pulses are reapplied every second, allows vortices to contribute more frequently to DBL destabilization during EDUF (Cournoyer et al., 2025). However, longer pauses observed in 5s/5s and 10s/10s allow for greater relaxation of the CP layer and restoration of concentration of charged peptides in the DBL, which reduces system resistance and improves current efficiency during the next pulse. Thanks to these opposing trends, the experimental data indicate that in most cases, all three conditions yielded comparable performance in terms of MR_{charge} in both compartments. This apparent paradox can be explained by considering the compensating effects of pulse and pause durations under the same α value. Although all three conditions share the same α and thus the same total time under voltage, the mechanisms driving mass transfer differ. 1s/1s promotes more frequent ECV while 5s/5s and 10s/10s enhance CP relaxation and DBL recovery. These opposing effects balance each other, leading to similar overall MR_{charge} despite the differences in pulse and pause durations. However, following the PCA analysis and MR_{charge} results, the 5s/5s condition outperformed both 1s/1s and 10s/10s. This could be explained by the interplay between CP during the pause and ECV activity during the pulse. Under 1s/1s, the short pause duration does not allow sufficient CP relaxation, so despite the frequent ECVs generation, their ability to enhance mass transfer is limited by the persistent polarization near the membrane. In contrast, under 10s/10s, the long pause allows full CP relaxation, but the long pulse interval reduces drastically the frequency of ECVs activation, diminishing their cumulative contribution. The 5s/5s condition achieves a better balance: the pause is long enough to partially dissipate CP while the pulse duration remains short enough to maintain frequent ECV activity. This optimal compromise would explain the higher migration efficiency and distinct clustering of 5s/5s observed in the PCA analysis.

The observed results in this study confirm and extend the hypothesis proposed (Cournoyer et al., 2024, 2025) that the electrical current modes strongly shape peptide migration in EDUF. However, whereas Cournoyer et al. grouped conditions into broad clusters (e.g., CC, PEF 10s/1s and PR 10s/1s showing similar selectivity), the present study using a wider range of PEF conditions revealed a finer structure in the peptide response. In the C_{RC}^{+}, three correlated clusters of peaks (groups A-C) emerged from the loading plot and the score plot separated multiple PEF conditions along PC1 and PC2; importantly, PC1 correlates negatively with duty cycle (α), indicating that lower α systematically favors higher peptide migration. The A_{RC}^{-} showed a simpler distribution, but the same general trend linking PC1 and α was observed. These results therefore reproduce the effect reported by Cournoyer et al. while demonstrating that the duty cycle (and not only a single combination of pulse and pause durations) is a robust, predictive descriptor of global migration behavior.

The pattern that emerges from this study supports a polarization-driven, competition-based mechanism in the DBL. In multicomponent systems, differences in electrophoretic mobility, diffusivity, and concentration establish a transport hierarchy that favors smaller, faster species under steady fields (Zimmermann et al., 2023). Under PEF, periodic pauses enable partial DBL relaxation, while the onset of each pulse generates a transient current surge and short-lived ECVs that enhance ion and peptide availability at the membrane surface as proposed by (Cournoyer et al., 2025). This dynamic explains why low α (e.g., more frequent pulses as in 1s/1s or relatively longer pauses as in 5s/5s and 10s/10s) were associated with higher overall migration: frequent re-application of the field produces more current surges/ECV events per unit time, mitigating CP and improving transport. In contrast, long pulses combined with short pauses (high α as in 10s/1s) reinforce a persistent DBL and promote steady-state selectivity favoring the low molecular weight and highly charged molecules and consequently these fastest species.

The observed selectivity shifts were restricted to a subset of peptides

(peaks 8, 11 and 18 in C^{+}_{RC} and peak 10 in A^{-}_{RC}), which were less strongly correlated with the reference clusters identified by PCA. These peptides appear to occupy a borderline position in the migration hierarchy: mobile enough to cross the membrane under certain conditions, but sensitive to transient changes in CP and DBL relaxation induced by PEF. In contrast, peptides tightly grouped with the reference clusters showed little or no selectivity variation, indicating that dominant fast-migrating species remain largely unaffected by pulse/pause cycling.

5. Conclusions

This study demonstrates that PEF conditions influence the efficiency and the selectivity of peptide migration. This was explained by the competitive nature of charge transport in multicomponent systems, where peptides and other charged species compete within the DBL. PEF modulates this competition, ultimately affecting which peptides are preferentially transported. These findings were explained based on the well-established mechanisms described in ED, where CP and ECVs are known to significantly influence ion transport. Building on the mechanisms previously proposed for EDUF by (Cournoyer et al., 2025), the present study supports the hypothesis that polarization-driven phenomena also influence peptide migration under PEF conditions. Our findings contribute to a deeper understanding of how these mechanisms can be used to enhance both separation efficiency and selectivity. Based on these observations, from the operational perspective, if the objective is the efficiency of peptide migration, low α conditions are recommended. This is because the efficiency in PEF regime strongly depends on the duty cycle, therefore, the shorter the pulse/pause ratio (Table 1), the higher the efficiency of mass transfer, which is consistent with the results observed in ED for salt demineralization (Mishchuk et al., 2001; Nikonenko et al., 2010).

Future work will focus on a thorough analysis of the effects of the considered PEF conditions on peptide migration. A comprehensive study employing a machine learning approach is currently underway to explore the migration behavior of the peptide population involved in the process, including all peptides, both migrating and non-migrating peptides. This analysis will consider all the physicochemical characteristics of the peptides, providing deeper insights into the peptide features influencing their migration and the associated phenomena.

CRediT authorship contribution statement

Leonel C. Mafotang T.: Writing – review & editing, Writing – original draft, Visualization, Validation, Methodology, Investigation, Formal analysis, Data curation, Conceptualization. **Aurore Cournoyer:** Writing – review & editing, Validation, Methodology, Investigation, Formal analysis, Data curation. **Jacinthe Thibodeau:** Writing – review & editing, Validation, Software, Formal analysis, Data curation. **Marcello Fidaleo:** Writing – review & editing, Writing – original draft, Visualization, Validation, Supervision, Methodology, Investigation, Funding acquisition, Data curation, Conceptualization. **Laurent Bazinet:** Writing – review & editing, Writing – original draft, Visualization, Validation, Supervision, Resources, Project administration, Methodology, Investigation, Funding acquisition, Data curation, Conceptualization.

Declaration of competing interest

The authors declare that they have no known competing financial interests or personal relationships that could have appeared to influence the work reported in this paper.

Acknowledgments

Acknowledgment is given to the Natural Sciences and Engineering Research Council of Canada (NSERC) for its financial support through the NSERC Discovery Grants Program (Grants RGPIN-2024-03929 to Laurent Bazinet). This publication was produced during the PhD program in Science, Technology and Biotechnology for Sustainability at the University of Tuscia, 38th cycle, with the support of a scholarship funded by Ministerial Decree No. 351 of April 9, 2022, under the National Recovery and Resilience Plan (NRRP) – funded by the European Union – NextGenerationEU – Mission 4 "Education and Research," Component 1 "Enhancement of education services: from early childhood to university" – Investment 3.4 "Advanced university education and skills". The authors express gratitude to Diane Gagnon from Laval University for her technical assistance in protein analyses.

Data availability

Data will be made available on request.

References

Aider, M., Brunet, S., & Bazinet, L. (2008). Electroseparation of chitosan oligomers by electrodialysis with ultrafiltration membrane (EDUF) and impact on electrodialytic parameters. *Journal of Membrane Science, 309*(1–2), 222–232. https://doi.org/10.1016/J.MEMSCI.2007.10.029

Alavi, F., & Ciftci, O. N. (2023). Purification and fractionation of bioactive peptides through membrane filtration: A critical and application review. *Trends in Food Science & Technology, 131*, 118–128. https://doi.org/10.1016/j.tifs.2022.11.024. November 2022.

Arrutia, F., Rubio, R., & Riera, F. A. (2016). Production and membrane fractionation of bioactive peptides from a whey protein concentrate. *Journal of Food Engineering, 184*, 1–9. https://doi.org/10.1016/j.jfoodeng.2016.03.010

Bazinet, L., & Firdaous, L. (2013). Separation of bioactive peptides by membrane processes: Technologies and devices. *Recent Patents on Biotechnology, 7*(1), 9–27. https://doi.org/10.2174/1872208311307010003

Bazinet, L., & Geoffroy, T. R. (2020). Electrodialytic processes: Market overview, membrane phenomena, recent developments and sustainable strategies. *Membranes, 10*(9), 221. https://doi.org/10.3390/membranes10090221

Belfort, G. (2019). Membrane filtration with liquids : A global approach with prior successes , new developments and unresolved challenges. *Angewandte Chemie International Edition, 58*, 1892–1902. https://doi.org/10.1002/anie.201809548

Buchanan, D., Martindale, W., Romeih, E., & Hebishy, E. (2023). Recent advances in whey processing and valorisation: Technological and environmental perspectives. *International Journal of Dairy Technology, 76*(2), 291–312. https://doi.org/10.1111/1471-0307.12935

Caetano-silva, M. E., Bertoldo-pacheco, M. T., Paes-leme, A. F., & Maria, F. (2015). Iron-binding peptides from whey protein hydrolysates : Evaluation , isolation and sequencing by LC – MS/MS. *Food Research International, 71*, 132–139. https://doi.org/10.1016/j.foodres.2015.01.008

Cournoyer, A., Bazinet, M., Clément, J.-P., Plante, P.-L., Fliss, I., & Bazinet, L. (2025). How peptide migration and fraction bioactivity are modulated by applied electrical current conditions during electromembrane process separation: A comprehensive machine learning-based peptidomic approach. *Food Research International, 200*, Article 115417. https://doi.org/10.1016/j.foodres.2024.115417

Cournoyer, A., Daigle, G., Thibodeau, J., Perreault, V., & Bazinet, L. (2024). Effects of applied current modes on the migration selectivity of peptides from a porcine cruor hydrolysate during electrodialysis with ultrafiltration membrane. *Separation and Purification Technology, 338*, Article 126280. https://doi.org/10.1016/j.seppur.2024.126280. January.

Cowan, D. A., & Brown, J. H. (1959). Effect of turbulence on limiting Current in electrodialysis cells. *Industrial & Engineering Chemistry, 51*(12), 1445–1448. https://doi.org/10.1021/ie50600a026

Damen, D., Thibodeau, J., Gaaloul, S., Fliss, I., Labrie, S., Hamoudi, S., & Bazinet, L. (2024). Influence of enzymatic hydrolysis conditions on antimicrobial activities and peptide profiles of milk protein-derived hydrolysates from white wastewater. *Cleaner Waste Systems, 9*, Article 100172. https://doi.org/10.1016/j.clwas.2024.100172. September.

Dushkova, M., Ivanova, M., Trublet, L., Petkova, Z., Teneva, O., Miteva-Petrova, M., Desseva, I., & Mihaylova, D. (2023). Flux behaviour, rejection and concentration factors, and energy demand during ultrafiltration of sweet buttermilk. *Applied Sciences, 13*(6), 3804. https://doi.org/10.3390/app13063804

Faucher, M., Geoffroy, T. R., Thibodeau, J., Gaaloul, S., & Bazinet, L. (2022). Semi-Industrial production of a DPP-IV and ACE inhibitory peptide fraction from whey protein concentrate hydrolysate by electrodialysis with ultrafiltration membrane. *Membranes, 12*(4). https://doi.org/10.3390/membranes12040409

Fernández, A., Suárez, A., Zhu, Y., FitzGerald, R. J., & Riera, F. A. (2013). Membrane fractionation of a β-lactoglobulin tryptic digest: Effect of the pH. *Journal of Food Engineering, 114*(1), 83–89. https://doi.org/10.1016/j.jfoodeng.2012.07.030

Geoffroy, T. R., Bernier, M. E., Thibodeau, J., Francezon, N., Beaulieu, L., Mikhaylin, S., Langevin, M. E., Lutin, F., & Bazinet, L. (2022). Semi-industrial scale-up of EDUF technology for the electroseparation of bioactive cationic peptides: Impact of process parameters and cell configurations on eco-efficiency. *Journal of Membrane Science, 641*(August 2021), Article 119856. https://doi.org/10.1016/j.memsci.2021.119856

Geoffroy, T. R., Thibodeau, J., Faucher, M., Langevin, M. E., Lutin, F., & Bazinet, L. (2022). Relationship between feed concentration and bioactive cationic peptide recovery: Impact on ecoefficiency of EDUF at semi-industrial scale. *Separation and Purification Technology, 286*, Article 120403. https://doi.org/10.1016/j.seppur.2021.120403. December 2021.

Geraldes, V., & Afonso, M. D. (2010). Limiting current density in the electrodialysis of multi-ionic solutions. *Journal of Membrane Science, 360*(1–2), 499–508. https://doi.org/10.1016/J.MEMSCI.2010.05.054

Gorobchenko, A., Mareev, S., & Nikonenko, V. (2022). Mathematical modeling of monovalent permselectivity of a bilayer ion-exchange membrane as a function of Current density. *International Journal of Molecular Sciences, 23*(9), 4711. https://doi.org/10.3390/IJMS23094711/S1

Gu, Y., & Wu, J. (2013). LC – MS/MS coupled with QSAR modeling in characterising of angiotensin I-converting enzyme inhibitory peptides from soybean proteins. *Food Chemistry, 141*(3), 2682–2690. https://doi.org/10.1016/j.foodchem.2013.04.064

Guo, M. R., Fox, P. F., Flynn, A., & Kindstedt, P. S. (1995). Susceptibility of β-Lactoglobulin and sodium caseinate to proteolysis by Pepsin and trypsin. *Journal of Dairy Science, 78*(11), 2336–2344. https://doi.org/10.3168/jds.S0022-0302(95)76860-6

He, R., Girgih, A. T., Rozoy, E., Bazinet, L., Ju, X. R., & Aluko, R. E. (2016). Selective separation and concentration of antihypertensive peptides from rapeseed protein hydrolysate by electrodialysis with ultrafiltration membranes. *Food Chemistry, 197*, 1008–1014. https://doi.org/10.1016/j.foodchem.2015.11.081

Hernandez-Ledesma, B., Amigo, L., Recio, I., & Bartolomé, B. (2007). ACE-Inhibitory and Radical-Scavenging Activity of Peptides derived from -Lactoglobulin f (19 − 25). Interactions with Ascorbic Acid. *Journal of Agricultural and Food Chemistry, 55*, 3392–3397. https://doi.org/10.1021/jf063427j

Kadel, S., Daigle, G., Thibodeau, J., Perreault, V., Pellerin, G., Lainé, C., & Bazinet, L. (2021). How physicochemical properties of filtration membranes impact peptide migration and selectivity during electrodialysis with filtration membranes: Development of predictive statistical models and understanding of mechanisms involved. *Journal of Membrane Science, 619*. https://doi.org/10.1016/j.memsci.2020.118175. May 2020.

Langevin, M. E., Roblet, C., Moresoli, C., Ramassamy, C., & Bazinet, L. (2012). Comparative application of pressure- and electrically-driven membrane processes for isolation of bioactive peptides from soy protein hydrolysate. *Journal of Membrane Science, 403–404*, 15–24. https://doi.org/10.1016/J.MEMSCI.2012.02.005

Lemay, N., Mikhaylin, S., & Bazinet, L. (2019). Voltage spike and electroconvective vortices generation during electrodialysis under pulsed electric field: Impact on demineralization process efficiency and energy consumption. *Innovative Food Science & Emerging Technologies, 52*, 221–231. https://doi.org/10.1016/j.ifset.2018.12.004. September 2018.

Li-Chan, E. C. Y. (2015). Bioactive peptides and protein hydrolysates: Research trends and challenges for application as nutraceuticals and functional food ingredients. *Current Opinion in Food Science, 1*(1), 28–37. https://doi.org/10.1016/j.cofs.2014.09.005

Lytras, F., Psakis, G., Gatt, R., Cebrián, G., Raso, J., & Valdramidis, V. (2024). Exploring the efficacy of pulsed electric fields (PEF) in microbial inactivation during food processing: A deep dive into the microbial cellular and molecular mechanisms. *Innovative Food Science & Emerging Technologies, 95*, Article 103732. https://doi.org/10.1016/J.IFSET.2024.103732

Malek, P., Ortiz, J. M., Richards, B. S., & Schäfer, A. I. (2013). Electrodialytic removal of NaCl from water: Impacts of using pulsed electric potential on ion transport and water dissociation phenomena. *Journal of Membrane Science, 435*, 99–109. https://doi.org/10.1016/j.memsci.2013.01.060

Martí-Calatayud, M. C., Sancho-Cirer Poczatek, M., & Pérez-Herranz, V. (2021). Trade-Off between operating time and energy consumption in pulsed electric field electrodialysis: A comprehensive simulation Study. *Membranes, 11*(1), 43. https://doi.org/10.3390/membranes11010043

Mishchuk, N. A., Koopal, L. K., & Gonzalez-Caballero, F. (2001). Intensification of electrodialysis by applying a non-stationary electric field. *Colloids and Surfaces A: Physicochemical and Engineering Aspects, 176*(2–3), 195–212. https://doi.org/10.1016/S0927-7757(00)00568-9

Nikonenko, V. V., Pismenskaya, N. D., Belova, E. I., Sistat, P., Huguet, P., Pourcelly, G., & Larchet, C. (2010). Intensive current transfer in membrane systems: Modelling, mechanisms and application in electrodialysis. *Advances in Colloid and Interface Science, 160*(1–2), 101–123. https://doi.org/10.1016/J.CIS.2010.08.001

Nikonenko, V., Uzdenova, A., Kovalenko, A., & Urtenov, M. (2024). Theoretical Study of the influence of electroconvection on the efficiency of Pulsed Electric Field (PEF) modes in ED desalination. *Membranes, 14*(11). https://doi.org/10.3390/membranes14110225

Roblet, C., Doyen, A., Amiot, J., & Bazinet, L. (2013). Impact of pH on ultrafiltration membrane selectivity during electrodialysis with ultrafiltration membrane (EDUF) purification of soy peptides from a complex matrix. *Journal of Membrane Science, 435*, 207–217. https://doi.org/10.1016/j.memsci.2013.01.045

Rubinstein, I., & Zaltzman, B. (2000). Electro-osmotically induced convection at a permselective membrane. *Physical Review, 62*(2), 2238–2251. https://doi.org/10.1103/PhysRevE.62.2238

Ruiz, B., Sistat, P., Huguet, P., Pourcelly, G., Araya-Farias, M., & Bazinet, L. (2007). Application of relaxation periods during electrodialysis of a casein solution: Impact on anion-exchange membrane fouling. *Journal of Membrane Science, 287*(1), 41–50. https://doi.org/10.1016/J.MEMSCI.2006.09.046

Salam, M. A., & Rahman, Q. M. (2018). *Fundamentals of electrical circuit analysis*. Singapore: Springer.

Sistat, P., Huguet, P., Ruiz, B., Pourcelly, G., Mareev, S. A., & Nikonenko, V. V. (2015). Effect of pulsed electric field on electrodialysis of a NaCl solution in sub-limiting current regime. *Electrochimica Acta, 164*, 267–280. https://doi.org/10.1016/j.electacta.2015.02.197

Suwal, S., Amiot, J., Beaulieu, L., & Bazinet, L. (2016). Effect of pulsed electric fi eld and polarity reversal on peptide/amino acid migration , selectivity and fouling mitigation. *Journal of Membrane Science, 510*, 405–416. https://doi.org/10.1016/j.memsci.2016.03.010

Suwal, S., Rozoy, É., Manenda, M., Doyen, A., & Bazinet, L. (2017). Comparative Study of in situ and ex situ enzymatic hydrolysis of milk protein and separation of bioactive peptides in an electromembrane reactor. *ACS Sustainable Chemistry & Engineering, 5*(6), 5330–5340. https://doi.org/10.1021/acssuschemeng.7b00651

Tavares, T., Contreras, M., Amorim, M., Pintado, M., Recio, I., & Malcata, F. X. (2011). Peptides Novel whey-derived peptides with inhibitory effect against angiotensin-converting enzyme : In vitro effect and stability to gastrointestinal enzymes. *Peptides, 32*, 1013–1019. https://doi.org/10.1016/j.peptides.2011.02.005

Tekinalp, Ö., Zimmermann, P., Holdcroft, S., Burheim, O. S., & Deng, L. (2023). Cation exchange membranes and process optimizations in electrodialysis for selective metal separation: A review. *Membranes, 13*(6), 566. https://doi.org/10.3390/membranes13060566

Tian, M., Fang, B., & Jiang, L. (2015). Structure-activity relationship of a series of antioxidant tripeptides derived from β -Lactoglobulin using QSAR modeling. *Dairy Science & Technology, 95*, 451–463. https://doi.org/10.1007/s13594-015-0226-5

Uzdenova, A. M., Kovalenko, A. V., Urtenov, M. K., & Nikonenko, V. V. (2015). Effect of electroconvection during pulsed electric field electrodialysis. Numerical experiments. *Electrochemistry Communications, 51*, 1–5. https://doi.org/10.1016/j.elecom.2014.11.021

Wang, X., Chen, H., Fu, X., Li, S., & Wei, J. (2017). LWT - Food Science and Technology A novel antioxidant and ACE inhibitory peptide from rice bran protein : Biochemical characterization and molecular docking study. *LWT - Food Science and Technology, 75*, 93–99. https://doi.org/10.1016/j.lwt.2016.08.047

Wang, R., Zhang, J., Tang, C. Y., & Lin, S. (2022). Understanding selectivity in solute–solute separation: Definitions, measurements, and comparability. *Environmental Science & Technology, 56*(4), 2605–2616. https://doi.org/10.1021/acs.est.1c06176

Zabolotsky, V. I., Achoh, A. R., Lebedev, K. A., & Melnikov, S. S. (2020). Permselectivity of bilayered ion-exchange membranes in ternary electrolyte. *Journal of Membrane Science, 608*, Article 118152. https://doi.org/10.1016/J.MEMSCI.2020.118152

Zaky, A. A., Simal-Gandara, J., Eun, J.-B., Shim, J.-H., & Abd El-Aty, A. M. (2022). Bioactivities, applications, safety, and health benefits of bioactive peptides from food and By-Products: A review. *Frontiers in Nutrition, 8*, 1–18. https://doi.org/10.3389/fnut.2021.815640. January.

Zhu, J., Fan, X., Cheng, Y., Agarwal, R., Moore, C. M. V., & Chen, S. T. (2014). Chemometric analysis for identification of botanical raw materials for pharmaceutical use : A case Study using Panax notoginseng. *PLoS One, 9*(1), 1–10. https://doi.org/10.1371/journal.pone.0087462

Zimmermann, P., Tekinalp, Ö., Solberg, S. B. B., Wilhelmsen, Ø., Deng, L., & Burheim, O. S. (2023). Limiting current density as a selectivity factor in electrodialysis of multi-ionic mixtures. *Desalination, 558*, Article 116613. https://doi.org/10.1016/j.desal.2023.116613. April.

Biosynth AG. (n.d.). *Peptide property calculator*. [Online Tool]. Biosynth. Retrieved September 30, 2024, from https://www.biosynth.com/tools/peptide-property-calculator.

NovoPro Bioscience Inc. (n.d.). *Peptide property calculator*. [Online Tool]. NovoPro Retrieved September 30, 2024, from https://www.novoprolabs.com/tools/peptide-property-calculator.